INVESTIGATION INTO THE MIXING LAYER DUE TO TWO PARALLEL SUPERSONIC STREAMS

Alexandre Z. TARNOPOLSKY and Sudhir L. GAI
University College, University of New South Wales,
Australian Defence Force Academy,
Canberra, A.C.T., Australia

Abstract

The mixing layer between supersonic air stream and a supersonic parallel Helium jet was studied. Schlieren photographs of 100ns exposure time were used to take the 'frozen' images of the mixing layer. Using this technique, the large-scale structure in the shear layer were found. Helium jets do not produce a significant change in the shear layer. It is possible that Helium just fills the turbulent eddies in the shear layer without changing their structure. Employing this assumption, the method to calculate density gradients as a quantitative characteristic of the mixing process has been developed using the results from holographic interferometry. Holographic interferograms of the density distributions were taken for different nozzle shapes. Using experimental results a simple isentropic model to predict salient parameters such as convective velocity and convective Mach numbers of the mixing layer has been developed.

Introduction

Currently, there is an intense interest in developing a supersonic combustion ramjet (SCRAMJET) which is being considered as a possible propulsive system for Aerospace planes of the future. Improvement of quality of the mixture between fuel and air is important to minimize the length and weight of the SCRAMJET combustor[1-4].

However, at supersonic speeds, mixing between air and fuel is not easy and the problem is accentuated with increasing Mach number. Considerable effort is therefore being directed at ways of enhancing this mixing.

The expected outcomes of the current experimental study is to find the ways of increasing the mixing process. As a first step in his study, we look at the mixing of two co-flowing parallel supersonic streams, a high Mach number main stream, representing air, and a low Mach number stream representing the fuel from the injector. Such simple arrangement allows us to develop an isentropic model to predict salient parameters such as convective velocity and convective Mach numbers of the large-scale structure in the mixing layer as well as to develop a quantitative characteristic of the mixing process using the results from holographic interferometry.

Experimental Arrangement and Techniques

Experiments were conducted in a blow-down wind-tunnel in a Mach number 2.0 air flow, which represented the main stream, and a co-flowing parallel helium jet from an injector at a Mach number 1.2.The injector was located at the centre of the wind-tunnel test section and extended upstream beyond the throat so that the main flow was uniformly divided into two supersonic parallel streams. The injector whose thickness was 6mm had two sets of nozzles. One set had a single slot nozzle of dimensions 1.19x54 mm at the exit and a second one has 5 slot nozzles, each of dimensions 1.75x7.75mm with 4.25mm separation between them.

The test section of the wind-tunnel is 90mm wide and 155mm high with two round windows on the side walls. The existence only of the side windows required two models of the injector to be made: one model to observe a

side-view image of the mixing layer and second model to observe a spanwise-view. All the nozzles have the same Mach number 1.2 and both sets of nozzles produce the same mass flux. The wind-tunnel test section with the injector model to observe the spanwise-view of the mixing layer is shown in Fig.1 and the sets of injectors are shown in Fig.2.

All measurements were conducted with the wind-tunnel main stream stagnation pressure P_o=295$\pm$ 3kPa and the jet stagnation pressure P_{jo}=120$\pm$4kPa. The condition for the jet stagnation pressures were chosen so as to produce a static pressure at the exit of the injector [5] nearly equal to the static pressure in the external stream.

Schlieren System

An electric spark light source Schlieren system[6] was used to obtain Schlieren photographs of the flow. The spark duration was 200nsec. This enabled to obtain a so-called 'frozen' images which show details of the flow structure such as small scale turbulent eddies and large-scale structures. The images were collected in the complete darkness using ordinary photo plates.

Both spanwise-view and side-view images of the flow were obtained twice using horizontal knife edge to evaluate variations in density in spanwise direction and vertical knife edge to evaluate variations in density in transverse direction. The results of the Schlieren flow visualisation are shown in Figs.3, 4 and 5.

Holographic Interferometry

The holographic interferometry (HI) was also employed in addition to Schlieren flow visualisation technique. A Ruby laser pulsed light source with an optical set-up similar to Mach-Zehnder interferometer was used. Both Infinitive Fringes Interferogrammes (IFI) and Finite Fringes Interferogrammes (FFI) were obtained for the side-view and the spanwise-view injector models.The FFI was obtained introducing into the light path a thin hollow wedge filled with liquids[7]. The results of HI are shown in Figs.6 and 7.

Results and Discussion

Schlieren system

Figure 3 shows the side-view images, when the horizontal knife edge is sensitive to the transverse density gradient. It is possible to identify the jet and the mixing layer clearly. It is also seen that the potential core of the jet extends to along 12 to 14 jet heights in the case of the set with 5 slot nozzles, where for the set with single slot nozzle it is along 15 to 18 jet heights.

Figure 4 shows the side-view images of the flow with the vertical knife edge to evaluate variations in density in stream-wise direction. A distinguishable feature in these pictures is the large-scale elongated structures inclined roughly 45^o to the free stream direction which do not seem to be effected by the jet. The presence of the jet can be identified, however, through the micro-structure embedded in the large-scale formations. Also, while the spreading of the jet is quite perceptible in the 5 slot jets, it is not so with the single slot jet. These results appear to show that the jet, while not substantially changing the large-scale turbulent structures, simply fills the void in the eddies.

Figure 5, which shows the spanwise-views with the horizontal knife edge to evaluate variations in density in the transverse direction, once again reveals large-scale structures and finer scales within it. While the single slot jet seems to indicate uniform mixing, the 5 slot jets are clearly separated for a long while and indicate some sort of mixing between them only at the end of the picture

Holographic Interferometry

Holographic interferometry (HI) was also used to obtain local density variations in the mixing layer.

Figure 6, which shows the spanwise-view of FFI, clearly verify that the density is nearly constant in the spanwise direction and refractive index distribution can be approximated as a two dimensional. Therefore, a relationship between refractive index change and the number of shifted fringe lines can be used as[8]

$$n(x,y) - n_o = \frac{\lambda}{L} N(x,y), \qquad (1)$$

where n(x,y) is the refractive index at the point (x,y) when wind-tunnel is running; n_o is the reference refractive index when wind-tunnel is off; N(x,y) is the number of shifted fringe lines in the point (x,y); λ is the wavelength of the light; L is the width of the wind-tunnel test section.

As we mentioned above, that the jet, while not substantially changing the large-scale turbulent structures, simply fills the cord in the eddies, increasing the density of the mixing layer and producing brighter images. On this basis we assumed that the change of the refractive index in the mixing layer from n_s to n_m occurs only because of the presence of Helium in the shear layer. Employing the Gladstone - Dale relationship[8]

$$n(x,y) = k\,\rho(x,y) + 1, \tag{2}$$

the Helium density distribution can be calculated as

$$\rho_{He}(x,y) = \frac{n_m(x,y) - n_s(x,y)}{k_{He}}, \tag{3}$$

where ρ_{He} is the Helium density in the cross-section of the mixing layer, kg/m^3; k_{He} is the Gladstone-Dale constant for Helium, m^3/kg; $n_s(x,y)$ is the refractive index at the point (x,y) of the shear layer when wind-tunnel is running and Helium jet is off; $n_m(x,y)$ is the refractive index at the point (x,y) of the mixing layer when wind-tunnel is running and Helium jet is on.

To obtain the refractive index variations $n_s(x,y)$ in the shear layer, FFI images were taken once with Helium jet off during the wind-tunnel run.

Figure 7 shows the side-view FFI images for the three cases again. The straight lines of the FFI images in the mixing layer indicate that the density distribution can be approximated as a linear function

$$\rho(x,y) = \frac{d\rho(x,y)}{dy}\,y + \rho_o, \tag{4}$$

where $\frac{d\rho(x,y)}{dy}$ is the density gradient in the cross-wise direction.

The density distribution measurements gives large uncertainties in highly turbulent flow. On the other hand, the measurement of the density gradient $\frac{d\rho(x,y)}{dy}$, characterising the speed of the diffusion process, can be done with sufficient accuracy. To define the Helium density gradient from the FFI image we have developed the relationship as

$$\frac{d\rho_{He}}{dy} = \frac{\lambda}{L\,k_{He}}\left(d_{f_m}\tan(\alpha_m)C_{y_m} - d_{f_s}\tan(\alpha_s)C_{y_s}\right), \tag{5}$$

where α_m and α_s are the angles of inclination of the fringe lines in the FFI images of the mixing layer and in the FFI images of the shear layer; d_{f_m} and d_{f_s} are the fringe line frequency, 1/mm; C_{y_m} and C_{y_s} are the y-scale coefficients of FFI images.

Figure 8 shows the result of the density gradient measurements for the three flow configurations. It is seen that the higher density gradient with single slot nozzle indicates more rapid helium diffusion into the shear layer than with 5 slot nozzles. However, with both single and multi-slot jets, this speed of the diffusion process becomes equal to the shear layer density gradient after 18 injector heights. It seems that the shear layer density gradient dominates after that point.

Theoretical development and discussion

The results from the flow visualization techniques can be summarised in the schematic (see Fig.9) of the topology of the mixing layer. From the flow visualisation studies it is seen that the flow consists of an external supersonic steam and a parallel jet separated by a shear layer of the injector. However, as a first step, this complicated flow may be approximated by two supersonic parallel streams one representing the external stream and one representing the jet (see Fig.10). The mixing between these two streams should give a reasonable picture of the physics of the flow sufficiently away from the edge of the injector. These simplifications allowed to develop a simple model to predict salient parameters such

as convective velocity and convective Mach numbers of the mixing layer.

The model has been developed for the mixing layer resulted from mixing of two parallel supersonic streams with unlimited thickness. The mixing process is assumed to start from the end of a splitter plate which divides the two streams.

According to the theory of a fully turbulent mixing layer, the so called 'wedge' of the mixing layer is assumed to grow linearly. Assuming a homogeneous structure of the mixing layer and according to the simple two-dimensional model of mixing layers (see Fig.10), if one chooses the streamline n-n' from the jet to meet the upper edge of the mixing layer at some point n' and then project it to the dividing streamline extending this to the lower edge of the mixing layer, one could locate a point such as m' which specifies the streamline m-m' from the upper stream.

The model is based on the assumption that mass and momentum fluxes (MMF) passing through the cross section between these two streamlines do not change from the edge of the injector to the point where they meet the mixing layer. We can therefore write equations, representing conservation of mass and momentum laws between these two streamlines as

$$\int_{0}^{y_1}\rho_1 U_1 dy+\int_{-y_2}^{0}\rho_2 U_2 dy=\int_{-y_{c2}}^{y_{c1}}\rho U dy, \tag{6a}$$

$$\int_{0}^{y_1}(p_1+\rho_1 U_1^2)dy+\int_{-y_2}^{0}(p_2+\rho_2 U_2^2)dy=\int_{-y_{c2}}^{y_{c1}}(p+\rho U^2)dy, \tag{6b}$$

where y_1, y_2, y_{c1} and y_{c2} are as defined in Fig.5. Assuming a free stream condition in the both streams, and keeping the same static pressure, Eqs.6a, 6b can be simplified as

$$\rho_1 U_1 y_1+\rho_2 U_2 y_2=\int_{-y_{c2}}^{y_{c1}}\rho U dy, \tag{7a}$$

$$y_1(p+\rho_1 U_1^2)+y_2(p+\rho_2 U_2^2)=\int_{-y_{c2}}^{y_{c1}}(p+\rho U^2 dy), \tag{7b}$$

Bogdanoff[9] and later Papamoschou & Roshko[10] introduced the concept of convective Mach numbers of the large-scale structure in the mixing layer. They assume that there exists a stagnation point between the two streams in the mixing layer and when they meet each other isentropically, their total pressure is nearly the same. The velocity at this point is called a convective velocity U_c.They developed the relationship between convective Mach numbers M_{c_1} and M_{c_2} as

$$M_{c_1}=\sqrt{\frac{\gamma_1}{\gamma_2}}\,M_{c_2}\,; \tag{8}$$

where γ_1 and γ_2 are the ratios of specific heats.

Later, Papamoschou[11] conducted a series of experiments where he determined the convective velocity of large-scale structures. In these experiments, he found that the experimental convective Mach numbers M_{c_1} and M_{c_2} are close to the Bogdanoff's model (see Eq.8) only when $M_c< 0.5$. The convective velocity of the large scale structure is closer to lower velocity when two supersonic flows mix and the convective velocity is closer to higher velocity when supersonic flow mixes with subsonic flow.

The results from the present experiments indicate existence of the large-scale structure. Assume that the whole structure moves with constant convective velocity U_c[11]. With the assumptions about the parallel flow and the same static pressure in the both streams ($p_1=p_2=p$), the dividing streamline is parallel to the splitter plate and $y_1=y_{c1}$, $y_2=y_{c2}$.

As discussed by Dimotakis[12], the dividing streamline separates the mixing layer into two unequal parts. Using Dimotakis' definition of shear-layer orientations, the angle-ratio of the unsymmetrical mixing layer could be written as

$$E_\alpha=\frac{\tan\alpha_1}{\tan\alpha_2}, \tag{9}$$

where $\tan\alpha_1=\frac{y_{c1}}{x_c}$, $\tan\alpha_2=\frac{y_{c2}}{x_c}$.

Finally, using non-dimensional ratios

$$r=\frac{U_2}{U_1},\ s=\frac{\rho_2}{\rho_1},\ s_c=\frac{\overline{\rho_c}}{\rho_1}\ \text{and}\ r_c=\frac{U_c}{U_1}$$

and the above assumptions, the Eqs.7 can be rewritten in the non-dimensional form as

$$E_\alpha + rs = s_c r_c \left(1+E_\alpha\right), \tag{10a}$$

$$\left(1+\gamma_1 M_1^2\right)E_\alpha+\left(1+\gamma_2 M_2^2\right) = \left(1+s_c r_c^2 \gamma_1 M_1^2\right)\left(1+E_\alpha\right), \tag{10b}$$

where $\overline{\rho}_c$ is the average density which can be calculated as

$$\overline{\rho}_c(y_{c1}+y_{c2}) = \int_{-y_{c2}}^{y_{c1}} \rho_c dy, \tag{11}$$

The unknown quantities in the Eqs.10 are r_c, s_c. However, the investigations of shear layer behaviour[13] and mixing layer growth rate[14] show that the density profile across layers depends on the velocity profiles. It is therefore proposed that the average density $\overline{\rho}_c$ depends on the convective velocity U_c, and this dependency is based on the assumption that the difference between $\overline{\rho}_c$ and ρ_m is proportional to the difference between U_c and U_m. In non-dimensional form it could be expressed as

$$\frac{s_c - s_m}{1 - s} = K \frac{r_c - r_m}{1 - r}, \tag{12}$$

where $s_m = \frac{1+s}{2}$ and $r_m = \frac{1+r}{2}$, K is the coefficient of proportional. Calculations have shown that the best fitting of Eq.12 to the experimental data occurs with K from 0.68 to 0.7.

Substituting s_c from the Eq.12 and E_α from the Eq.10a into the Eq.10b, we can obtain a third order equation for convective velocity ratio r_c

$$r_c^3 + a\, r_c^2 + b\, r_c + c = 0, \tag{13}$$

where the coefficients a, b and c are the functions of velocity and density ratios r and s and of the coefficient of proportional K from the Eq.12.The convective Mach numbers M_{c1} and M_{c2} can then be calculated using the solution for r_c from the Eqs.13, viz.

$$M_{c1}=M_1(1-r_c) \tag{14a}$$

$$M_{c2}=M_2\left(\frac{r_c}{r} - 1\right) \tag{14b}$$

Of course, for the jet with limited thickness MMF model can be used only up to the cross-section where jet potential core is ended.Using the present density measurements from the holographic interferometry, the convective Mach numbers were calculated for 1 slot and 5 slot jets employing Eqs.12. MMF model has been used also to calculate the convective Mach numbers for Papamoschou's[11] experiments. The predicted convective Mach numbers together with the experimental results are shown in Fig.11. The experimental and theoretical results for the same case are joined by broken lines[11]. The calculated convective Mach numbers coincide well with 1 slot jet experimental convective Mach numbers and shows big discrepancy with 5 slot jets. Looking on the top view Schlieren images of the 5 slot jets, we can see that the 5 jets have some expansion in the spanwise direction. It is possible that two-dimensional assumption is not appropriate for this case. This is how the discrepancy can be explained. However, the MMF model shows still better result compare with Bogdanoff's model even for 5 slots.

The analysis of the calculations for all experimental conditions has shown that for the convective Mach numbers smaller then $M_c<0.3$ the present MMF model and the Bogdanoff's model give good agreement with the experiments (see Fig.11).We also note that for the convective Mach numbers $0.3 < M_c < 0.5$ the MMF model yields values close to experimental result although agreement is not very good. However, it still show the tendency to move towards the experimental results.

Significant improvement of the present MMF model over the Bogdanoff's model happens for the convective Mach numbers larger then $M_c > \frac{1}{\sqrt{2}}$.

The MMF model allows also to calculate the length of potential cores of the jets. The measured length of the jet potential core of the jet extends to along 12 to 14 jet heights in the case of the set with 5 slot nozzles, where for the set with single slot nozzle it is along 15 to 18 jet heights.

The calculated length for 1 slot jet is 17.1 which is close enough with experimental results. The calculated length for 5 slot jets is 23.3 which is too far from experimental results. We mentioned before why this discrepancy could happen.

Conclusions

The mixing layer between two parallel supersonic streams has been studied experimentally and theoretically. The experimental study shows that the shear layer density gradient dominates in the mixing layer over 18 injector heights. It seems that the control of the mixing layer over this distance can be done by regulating the behaviour of the shear layer only.

It has been shown that for two-dimensional mixing layer the present MMF model gives good agreement with the experiments. The calculations were done from subsonic to supersonic convective Mach numbers higher than $M_c > \frac{1}{\sqrt{2}}$ using isentropic assumptions and without considering the effect of shock waves. It seems that for two parallel supersonic streams the isentropic model can still be used to predict the convective velocity and convective Mach numbers.

References.

1. T.G.Tillman, W.P.Patrick and R.W.Paterson, "Enhanced Mixing of Supersonic Jet", *Journal of J. Propulsion,* Vol.7, No.6, 1991, pp.1006-1014.

2. D.S.Dolling, E.Fournier and Y.R.Shau, "Effects of Vortex Generators on the Growth of a Compressible Shear Layer", *Journal of Propulsion and Power*, Vol.8, No.5, 1992, pp.1049-1056.

3.E.M.Fernandos and S.Menon,"Mixing Enhancement in Compressible Mixing Layers: An Experimental Study", *AIAA Journal,* Vol.31,No.2,1993,pp.278-285.

4.R.R.Kumar, J.Kurian "Studies on Freejets from Radial Lobed Nozzles", *Experiments in Fluids* 19 (1995), pp.95-102.

5. Magi E. C., "Investigations into the Flow behind Castellated Blunt Trailing Edge Aerofoils at Supersonic Speed."*Ph.D. Thesis. Dept. of Aerospace and Mechanical Engineering, The University of New South Wales, 1990.*

6. Manual of Multiple Spark Camera Chronolite 8, *IMPULSPHYSIK GMBH Hamburg*,1977.

7. Ostrovsky, Butusou, Ostrovskaya (1980), Interferometry by Holography, *Springer Series in Optical Sciences, Vol.20, pp.157.*

8. Holographic Interferometry by C. M. Vest, *John Wiley & Sons*, New York, 1979, pp.311-329.

9.Bogdanoff D. W. (1986) "Compressibility Effects in Turbulent Shear Layer." *AIAA Journal Vol.21, No.6, 1983, pp.926-927.*

10. Paramoschou D. & Roshko A. (1988), "The compressible turbulent shear layer: an experimental study." *J. Fluid Mech., Vol.197, pp.453-477.*

11. Papamoschou D.(1991) "Structure of the Compressible Turbulent Shear Layer."*AIAA Journal Vol.29, No.5, May 1991, pp.680-681.*

12. Dimotakis P.(1986), "Two-Dimensional Shear-Layer Entrainment." *AIAA Journal Vol.24, No.11, Nov.1986, pp.1791-1796.*

13. Tanner M. (1984) "Steady Base Flows." Prog.Aerospace *Sci. Vol.21, pp.81-157, 1984*

14. Brown G. and Roshko A. (1974) "On density effect and large structure in turbulent mixing layer." *J.Fluid Mech. (1974), Vol.64, part 4, pp.775-810.*

15. Tarnopolsky A. Z. & Gai S. L. (1995), "Investigation into the Mixing Layer due to Two Parallel Supersonic Streams", *Dept. Rept., ADFA, Canberra,May,1995.*

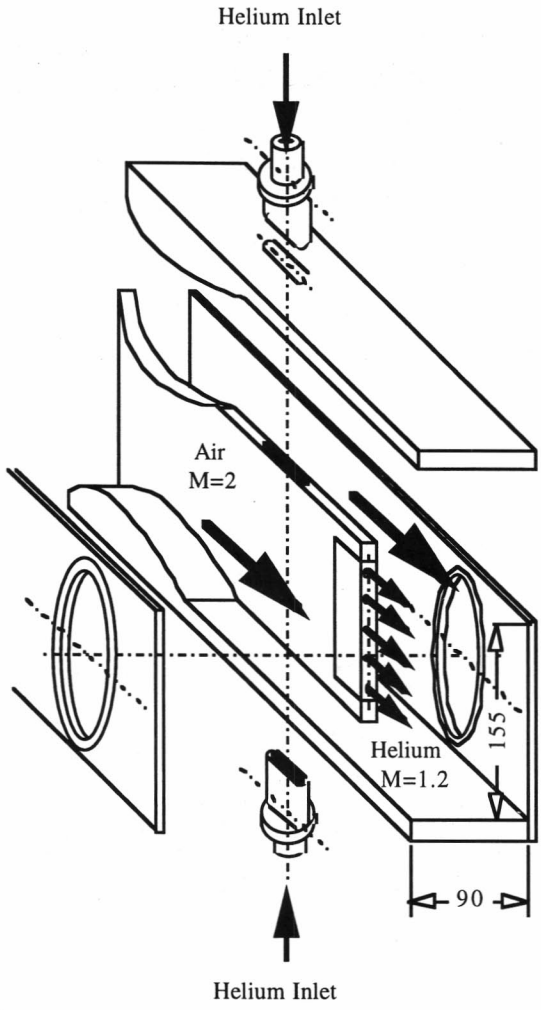

Fig.1 Exploded view of the test section with injector model to observe spane-view images of the mixing layer.

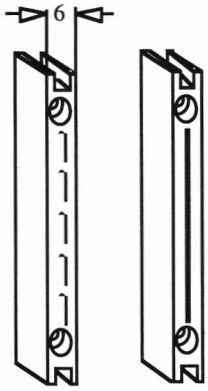

a) b)

Fig.2 Changeable sets of nozzles .
a - set of 5 slot nozzles;
b - set of a single slot nozzle.

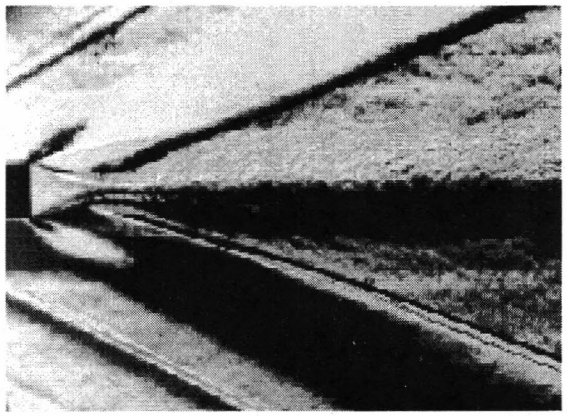

a) shear layer with jet off

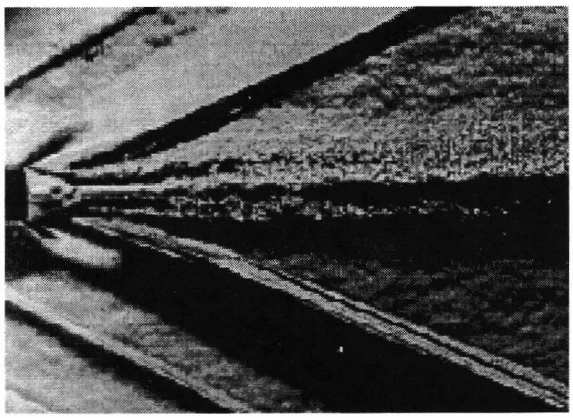

b) mixing layer with 1 slot jet on

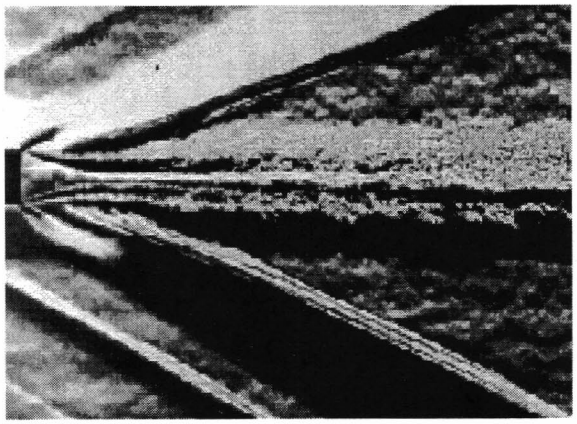

c) mixing layer with 5 slots jet on

Fig.3 Spanwise-view Schlieren images with horizontal knife edge. Flow goes from left to right

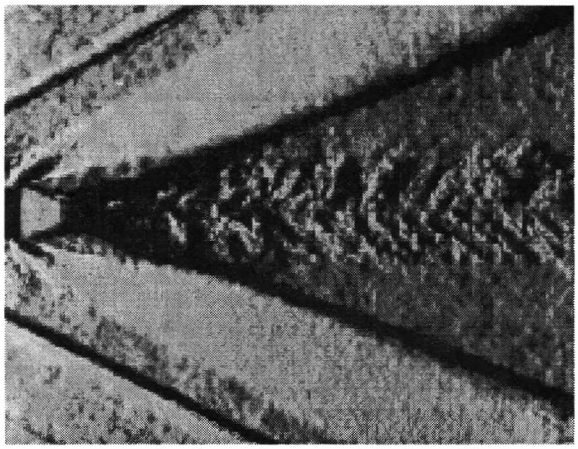

a) shear layer with jet off

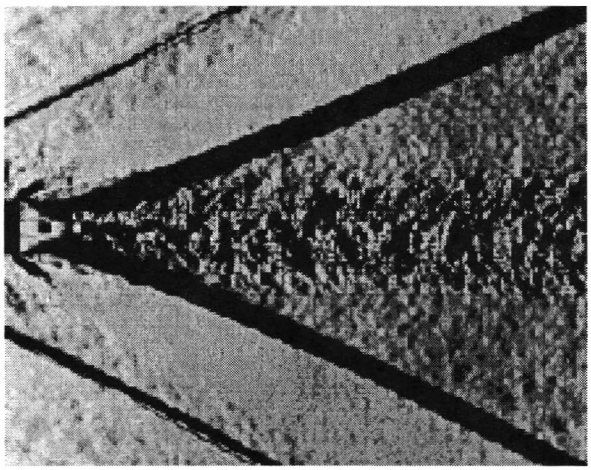

b) mixing layer with 1 slot jet on

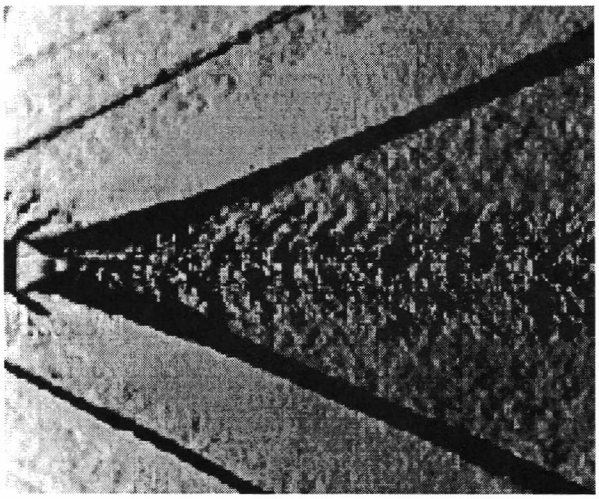

c) mixing layer with 5 slots jet on

Fig.4 Side-view Schlieren images with vertical knife edge. Flow comes from left to right

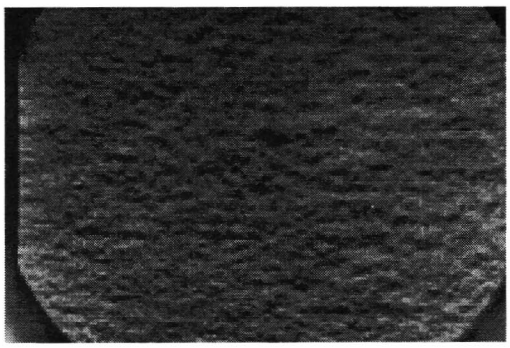

a) share layer with jet off

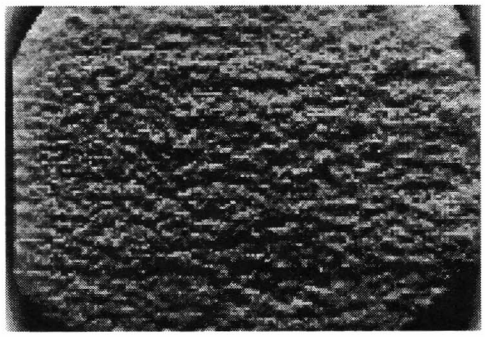

b) mixing layer with 1 slot jet on

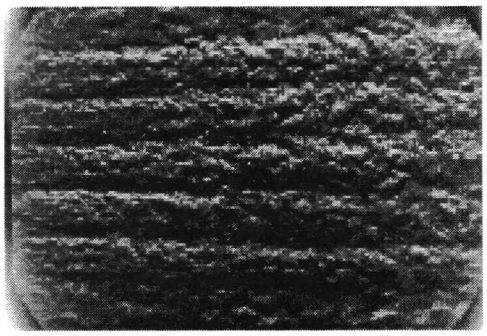

c) mixing layer with 5 slots jet on

Fig.5 Spanwise-view Schlieren images with horizontal knife edge. Flow comes from left to right

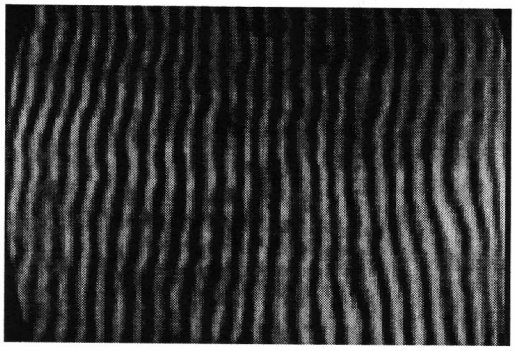

a) shear layer with jet off

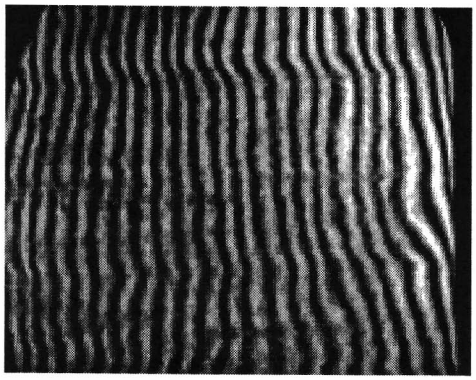

b) mixing layer with 1 slot jet on

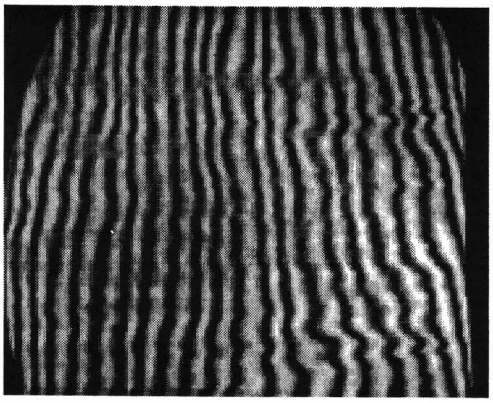

c) mixing layer with 5 slots jet on

Fig.6 Spanwise-view images of finite fringes holographic interferogramms. Flow goes from right to left.

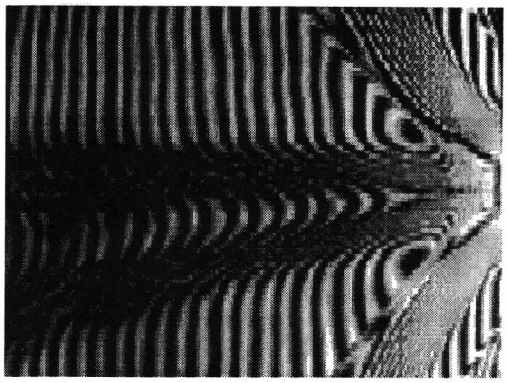

a) shear layer with jet off

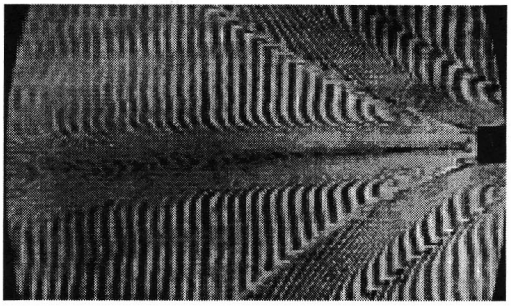

b) mixing layer with 1 slot jet on

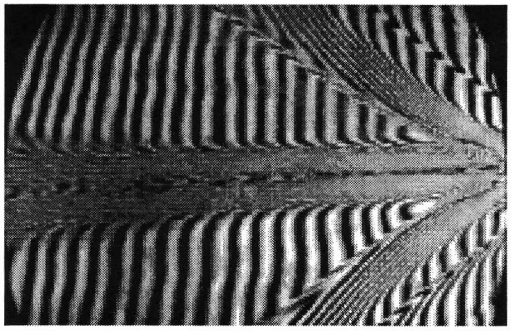

c) mixing layer with 5 slots jet on

Fig.7 Side-view images of finite fringes holographic interferogramms. Flow goes from right to left.

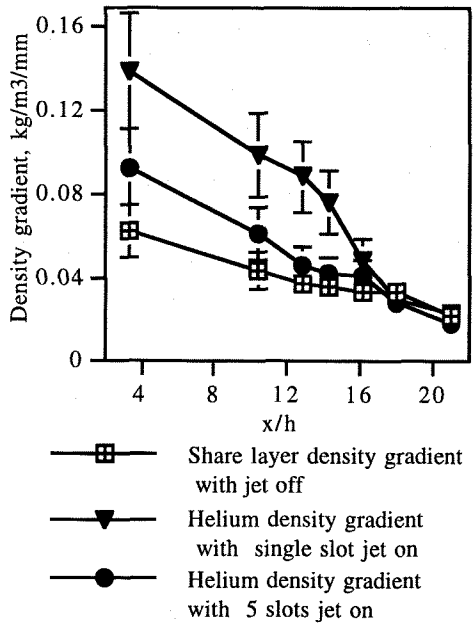

Fig.8 Density gradient in the stream-wise direction.

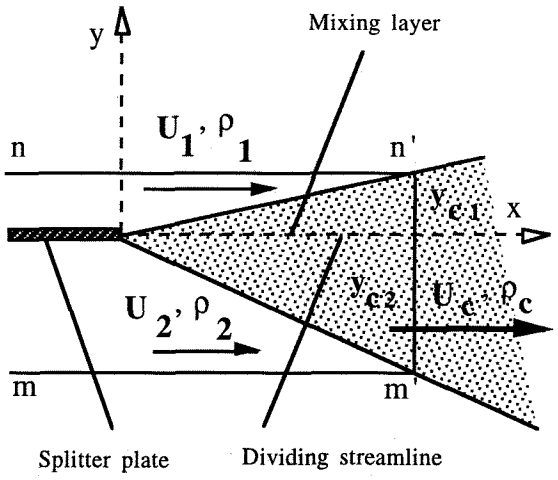

Fig.10 Schematic of simplified mixing layers.

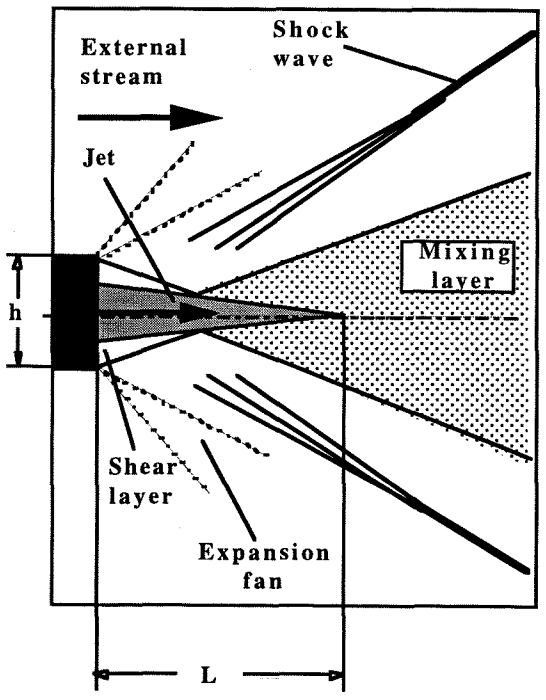

Fig.9 Schematic of the mixing layer behind injector, where h is the height of the injector; L is the length of jet potential core.

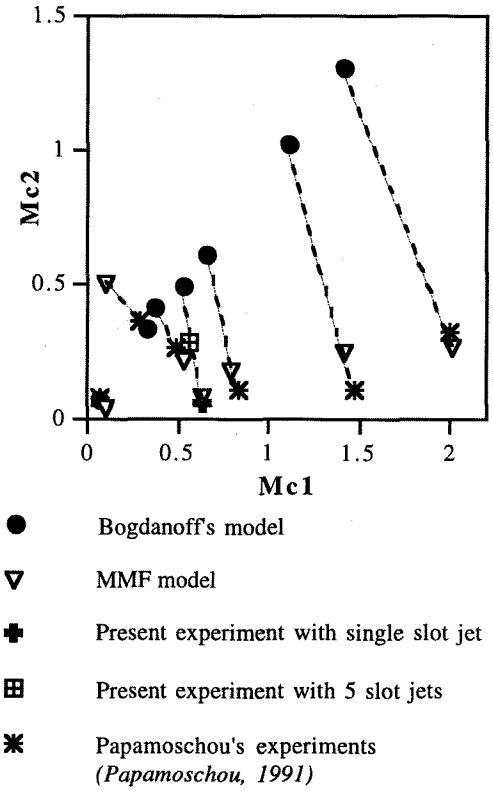

Fig.11 Experimental and calculated convective Mach numbers.